IJCRT.ORG ISSN : 2320-2882

INTERNATIONAL JOURNAL OF CREATIVE RESEARCH THOUGHTS (IJCRT)

An International Open Access, Peer-reviewed, Refereed Journal

AN EXTENSIVE ANALYSIS OF CLASSIFICATIONMETHODOLOGIES USED IN BCI: A SURVEY.

HEMANTH C,Dr RAVIKUMAR A V(Assosiate profssor at SJBIT), SACHIN R, AISHWARYA C R, JAHNAVI H V

Department of Electronics & Communication,SJB Institute of Technology, Bengaluru, India

Abstract: This BCI systems are able to communicate directly between the brain and computer using neural activity measurementswithout the involvement of muscle movements. By measuring cerebral activity, brain-computer interfaces (BCIs) can establish direct communication between the brain and computer without requiring the use of muscles. They are very important for those with severe disabilities, but before they are widely used, we must investigate how well they function in long-term real-world settings. It's also critical to figure out realistic ways to share these technologies with others. Furthermore, it is important to enhance the performance robustness of BCI systems to a degree equivalent to that of naturally occurring muscle-based health monitoring. Ensuring BCI systems are as dependable as regularly monitoring your health through muscle movements is a major challenge. Weshall review recent research in this paper.

Keywords- BCI, EEG, SSVEP, CNN, KNN, CCA, SVM

I. INTRODUCTION

Over the last 10 years, brain–computer interface (BCI) has become a promising technology that uses electroencephalogram (EEG) signals to translate mental activity into commands. People who are paralyzed can now converse mentally thanks to modern technology. BCI creates a direct communication channel between a person and a machine as an alternative to the traditional communication channels, which rely on peripheral nerves and muscles [8]. The creation of BCIs was viewed as science fiction until recently. A brain-computer interface (BCI) system enables the brain to work in tandem with an external device to execute tasks like moving a computer cursor, robotic arm, or wheelchair by using impulses from the brain. A BCI model consists of four key parts: the filter, the amplifier, the control system, and the sensing device. The sensing device comprises a cap consisting of the electrodes which are placed according to the international 10–20 standards [3, 4]. In BCI, when someone thinks about performing a task, like moving a cursor, the signals generated in the brain aren't sent to the finger on a computer's mouse through the body's neuromuscular system. Instead, these signals are directed to an external device that decodes them, facilitating actions such as cursor movement. The scope of BCI research extends to assisting individuals with hearing, sight, and movement impairments. Globally, approximately
1.5 billion people grapple with neurological and neuroanatomical diseases, resulting in challenges related to independent communication, reaching, and grasping. A crucial component of BCI, the cortical prosthetic system involves an end effector. Thisend effector responds to commands transmitted via a BCI, which records the cortical activity of individuals coping with neurological dysfunctions like spinal cord injuries, amyotrophic lateral sclerosis, and strokes. The BCI decodes information associated with the intended function. The present landscape of BCI technology encompasses a diverse range of end effectors, from virtual typing communication systems to robotic arms and hands, including functional electrical stimulation for limb reanimation. This technological innovation holds promise for enhancing communication and

fostering independence among individuals facing neurological challenges.BCI technologies exhibit various degrees of invasiveness, diverse spatial and temporal resolutions, and the ability to record a wide range of signals. In applications like low-throughput communication spelling systems [5], non-invasive brain imaging technologies such as EEG, MEG, and fMRI are commonly employed. However, non-invasive BCI approaches have drawbacks. They can be slow, as seen in case of fMRI, have limited spatial resolution, and are susceptible to external artifacts [6]. Consequently, they are not suitable for demanding real-time applications, including high-performance communications, tracking multidimensional robotic limbs, or coordinating grasps and reaches in the reanimation of paralyzed limbs. On the contrary, invasive BCIs present distinct advantages. Their ability to command higher-dimensional systems and restore more complex functions is a result of their higher resolution and broader transmission bandwidth. This makes invasive BCIs better suited for handling intricate and real-time tasks compared to their non-invasive counterparts. In a similar vein, eye tracking emerges as a potential means for paralyzed individuals to control external devices. However, the technology has several drawbacks. It relies on cameras or electrodes placed on the face to capture eye movements or electrical signals, employing methods like electrooculography (EOG). Despite its promise, the reliance on external facial apparatus can be limiting, introducing challenges related to comfort, invasiveness, and practicality. With respect to Brain-Computer Interface (BCI), a transformative alternative is presented. BCI facilitates the translation of neural commands directly from the human brain into actions performed by external devices [7]. This innovative approach bypasses the need for external facial components, offering a potentially more seamless and user-friendly interaction between the user and the technology. Beyond its primary application in aiding individuals with motor system disorders, Brain-Computer Interface (BCI) technology proves beneficial for those with healthy motor systems and the elderly. The development of intelligent, adaptive, and rehabilitative BCI applications for adults and geriatric patients holds the potential to significantly enhance their quality of life. These applications can strengthen familial bonds, improve cognitive and motor skills, and aid in various household tasks. Contrary to the misconception of BCIs as mind-reading technologies, they operate on a collaborative basis with users. Unlike mind readers, BCIs empower users by interpreting brain signals instead of relying on muscle movements, ensuring that information is not extracted without consent. Through training sessions, users generate specific brain signals that inform the BCI of their intended actions. The BCI then translates these signals into instructions for the output device, facilitating seamless collaboration between the user and the technology Despite the promising prospects, the research community faces significant challenges in implementing BCI devices. Notably, there is a crucial emphasis on making electrodes and surgical methods minimally invasive. Consequently, extensive research is dedicated to non-invasive methods of brain-computer interfacing, aiming to refine the usability and accessibility of BCI technology for a broader user base.

II Related Works

In paper [1], The authors in this paper uses these methods for the classification of EEG

1. SVM

In addition to feature extraction, another considerably important issue is how to design a powerful classification algorithm for accurate recognition of EEG response to MI. A well-known benchmark algorithm, support vector machine (SVM) has been most widely adopted for MI-related EEG classification. SVM finds a hyperplane in a high dimension so that the maximum separation margin is achieved. This can be formulated as

$$L = \frac{1}{2}\|w\|^2 + C(\#\ of\ mistakes) \quad \text{[equation 1]}$$

In this case, the trade-off between maximizing the margin and minimizing errors is determined by the hyper parameter C. When C is small, the emphasis is more on maximizing the margin and less emphasis is placed on misclassification; conversely, when C is large, the emphasis is more on preventing misclassification at the expense of maintaining a small margin.

The concept is to create a slack variable, ξ_i, for each data point, x_i. If x_i is on the incorrect side of the margin, the value of □_iis the distance of x_i from the margin of the appropriate class; otherwise, it is zero. As a result, points that are far from the margin on the incorrect side would incur additional penalties.

With this idea, each data point **x_i** needs to satisfy the following constraint:

$$y_i(\vec{w}.\vec{x}_i + b) \geq 1 - \xi_i$$ [equation 2]

In this case, the left side of the inequality can be compared to the classification confidence. A confidence score of greater than one indicates that the classifier properly classified the point. Confidence scores less than 1, on the other hand, indicate incorrect point classification by the classifier, incurring a linear penalty of ξ_i.

Given these constraints, our objective is to minimize the following function:

$$L = \frac{1}{2}\|\vec{w}\|^2 + C\sum_i \xi_i + \sum_i \lambda_i(y_i(\vec{w}\ .\ \vec{x}_i + b) - 1 + \xi_i)$$ [equation 3]

wherein we have optimized the loss function under constraints using the ideas of the Lagrange multiplier. Let's contrast this with the goal of SVM, which deals with the cases that may be divided linearly (as stated below).

$$L = \frac{1}{2}\|\vec{w}\|^2 + \sum_i \lambda_i(y_i(\vec{w}.\vec{x}_i + b) - 1)$$

[equation 4]

It is evident that the amended aim retains all of the original phrases, with the exception of the ξ_ i terms. Generalized functions called kernel functions take two vectors as input (of any dimension) and return a score indicating the similarity between the input vectors. The dot product function is a basic Kernel function that you are already familiar with. If the dot product is little, we infer that the vectors are different, and if the dot product is large, we infer that the vectors are more similar.

Let us look at the objective function for the linearly separable case:

$$L = \sum_i \lambda_i - \frac{1}{2}\sum_i \sum_j \lambda_i \lambda_j y_i y_j \vec{x}_i.\vec{x}_j$$ [equation 5]

A Kernel function can be written mathematically as follows:

$K(x, y) = \ < \phi(x), \phi(y) >$

Kernel function transformation for two points P_1 and P_2.

$$K(P_1, P_2) =< \phi(x_1, y_1), \phi(x_2, y_2) >$$
$$K(P_1, P_2) = x_1^2 x_2^2 + y_1^2 y_2^2 + 2x_1 y_1 x_2 y_2$$ [equation 6]

[equation 7]

2. ELM

Huang first proposed the extreme learning machine (ELM) as an expansion of the single layer feedforward network. Without requiring repeated optimisation, ELM just uses the Moore–Penrose generalised inverse of a hidden matrix to determine the output weights given randomly initialised hidden node settings. ELM with L hidden nodes is modelled mathematically as

$$\sum_{j=1}^{L} \beta_j h_j(\mathbf{x}_i) = y_i, \quad i = 1, \ldots, N, \qquad (3)$$

where hj(xi) is a feature mapping for the jth hidden node output and bj is a weight connecting the output neurons to the jth hidden neuron. The sigmoid function is a mapping function that is frequently utilised.

$$h_j(\mathbf{x}_i) = \frac{1}{1 + \exp\left(-\left(\mathbf{w}_j^{\mathrm{T}}\mathbf{x}_i + b_j\right)\right)},$$

[equation 8]

where wj =transpose [wj1; ...; wide] belongs to R is a weight vector connecting the input neurons and the jth hidden neuron, and bj denotes the bias term.

$$\mathbf{H}\boldsymbol{\beta} = \mathbf{y}, \qquad (5)$$

with $\boldsymbol{\beta} = [\beta_1, \ldots, \beta_L]^{\mathrm{T}} \in \mathbb{R}^L$, $\mathbf{y} = [y_1, \ldots, y_N]^{\mathrm{T}} \in \mathbb{R}^N$ and

$$\mathbf{H}(\mathbf{w}_1, \ldots, \mathbf{w}_L, b_1, \ldots, b_L, \mathbf{x}_1, \ldots, \mathbf{x}_N) = \begin{bmatrix} h_1(\mathbf{x}_1) & \cdots & h_L(\mathbf{x}_1) \\ \vdots & \ddots & \vdots \\ h_1(\mathbf{x}_N) & \cdots & h_L(\mathbf{x}_N) \end{bmatrix} \in \mathbb{R}^{N \times L}, \qquad (6)$$

[equation 9]

where H stands for the output matrix of the hidden layer. In contrast to traditional learning algorithms, ELM may simultaneously minimise the output weights' smallest norm and the training error. Using wj and bj (j ¼ 1;; L), randomly initialised hidden node parameters

Methodology:

A comparative study was conducted to assess the performance of algorithms, namely SVM, ELM, BELM, and SBELM, in the classification of MI-related EEG. The evaluation involved training classifiers on 30%, 50%, and 80% of the samples for each subject. To be specific, 48 samples were randomly chosen for feature extraction and classifier training, leaving the remaining samples for testing. This process was repeated 100 times, and the average classification accuracy was computed.

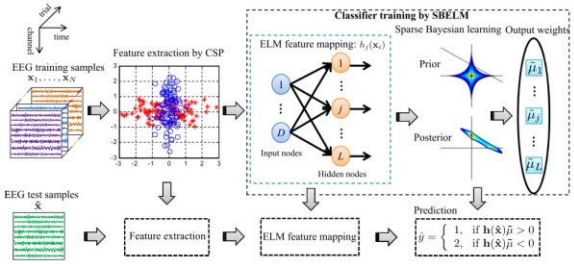

Fig: 1 [Illustration of the SBELM-based model for classification of motor imagery EEG]

Results:

Fof 30% of samples

Subject	SVM	ELM	BELM	SBELM
B0103T	76.5	76.9	**77.8**	**77.8**
B0203T	56.8	59.0	59.4	**61.9**
B0303T	51.6	51.8	**54.4**	54.1
B0403T	98.8	98.5	98.8	**99.1**
B0503T	83.6	84.3	84.3	**84.8**
B0603T	67.8	68.3	68.0	**69.3**
B0703T	83.1	83.8	84.1	**84.6**
B0803T	87.4	88.8	89.3	**90.9**
B0903T	81.5	82.3	**83.9**	83.6
Average	76.3 ± 15.1	77.1 ± 14.8	77.8 ± 14.5	**78.5** ± 14.3
p value	< 0.005	< 0.005	0.064	–

for 50% of samples

Subject	SVM	ELM	BELM	SBELM
B0103T	75.3	75.3	75.6	**76.2**
B0203T	54.8	55.0	55.4	**55.9**
B0303T	49.0	49.5	49.8	**50.1**
B0403T	97.1	97.4	97.6	**98.8**
B0503T	82.3	82.3	83.1	**83.4**
B0603T	64.0	64.6	65.3	**65.8**
B0703T	82.5	82.7	83.1	**84.2**
B0803T	85.3	85.7	86.9	**87.9**
B0903T	81.0	81.5	81.8	**82.3**
Average	74.6 ± 15.6	74.9 ± 15.3	75.4 ± 15.6	**76.1** ± 15.8
p value	< 0.001	< 0.001	< 0.001	–

for 80% of samples

Subject	SVM	ELM	BELM	SBELM
B0103T	75.8	76.1	76.5	**76.9**
B0203T	55.3	57.7	56.3	**57.6**
B0303T	49.5	50.3	51.1	**51.3**
B0403T	98.6	98.6	98.8	**99.0**
B0503T	82.3	83.6	84.0	**84.2**
B0603T	66.6	67.3	67.1	**67.5**
B0703T	83.1	83.6	83.6	**84.6**
B0803T	86.8	86.8	87.9	**89.1**
B0903T	81.5	82.1	**82.5**	**82.5**
Average	75.5 ± 15.7	76.2 ± 15.2	76.4 ± 15.5	**77.0** ± 15.4
p value	< 0.001	< 0.05	< 0.05	–

The authors in [1] have shown that extreme learning machine (ELM) is more efficient than SVM, considering the benchmark performance. Sparse Bayesian ELM based algorithm (SBELM) is shown to exhibit high characterization accuracy on EEG signals. During the comparative study, it is observed that accuracy of 76.3%, 77.1%, 77.8% and 78.5% is obtained via SVM, ELM, BELMand SBELM, respectively.

In paper [2] The used technologies in the above paper are as follows:

SSVEP Signals:

The experimentation in SSVEP-based BCI primarily explores flickering frequencies categorized as low (0-14Hz) and medium (15- 30Hz), both below 30 Hz. This choice is driven by the advantageous increase in amplitude for frequencies below 30 Hz compared to those exceeding 30 Hz . SSVEP stimuli are repetitive and fall into three distinct types: light stimuli, single graphic stimuli, and pattern reversal stimuli. This study places particular emphasis on light stimuli due to the observed heightened response compared to other stimulus sources. Among light stimuli, LEDs are the prevailing choice, further contributing to the diversity of stimulus sources in SSVEP-based BCI research.

Hilbert Transform

The uniqueness of this work is that, Hilbert Transform (HT) is applied to simulated EEG signal for phase extraction to control both simulated and real time robotic car simultaneously using LabVIEW and NI MyDAQ as a medium of interface. Upon phase identification, translational commands are then directed to robotic car wirelessly with the help of Radio Frequency (RF) transmission module working with a frequency of 434MHz. The commands are also passed to simulated robotic car in LabVIEW. For phase detection, the Fourier Transform of the input sequence X is computed as: Y = F{X}. Next, the DC component is set to zero: Y0 = 0.0. If the sequence Y is of an even size, the Nyquist component is set to zero, YNyq = 0. The positive harmonics and negative harmonics are multiplied by –j and j respectively. The new sequence is given by Hk = –j sgn (k) Yk . To obtain the Hilbert transform of X, the Inverse Fourier transform of H is

computed. The original signal and its Hilbert Transform are given as inputs to a "Re/Im to Polar" function which converts the rectangular components (real and imaginary part) of the inputs to corresponding polar coordinates, r and θ. The value θ gives the instantaneous phase of the input signal. Once the phase of the signal is detected, it is classified based on its value.

Methodology

In this work, a simulated multi-tone signal is generated and sampled at a rate of 8k samples per second, and band pass filtered for a frequency of 21 ± 0.5 Hz [10]. HT is then applied on the filtered signal for phase detection in LabVIEW as it is highly recommended for phase selectivity [13]. Depending on the quadrant in which it falls, a case number is assigned, ex: (First quadrant - 0 ◦ to 90◦ , Case 1; Second Quadrant - 91◦ to180◦ , Case 2; Third Quadrant - 181◦ to 270◦ , Case 3; Fourth Quadrant - 271◦ to 360◦ , Case 4). This case number is then passed from the LabVIEW program to the NI myDaq device, in the form of parallel data comprising of four bits, which indicate, the direction of movement of the robot car. A three dimensional robot car, comprising of a steering frame and four mecum wheels, simulated in LabVIEW. It can move forward in two directions (X direction and Y direction), based on the command given to it. Its angular velocity is set by the producer consumer model in the LabVIEW program

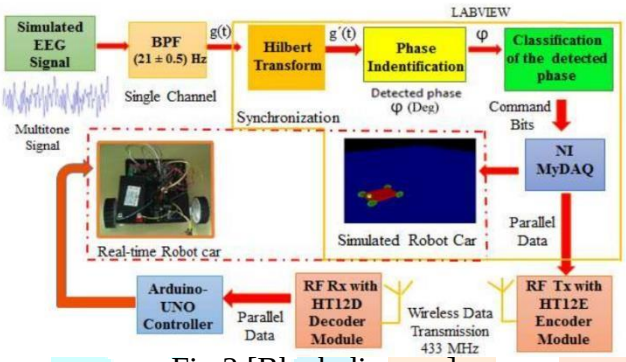

Fig:2 [Block diagram]

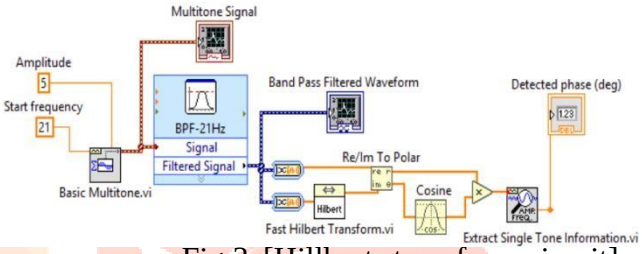

Fig:3 [Hillberts transform circuit]

Sl. No.	Phase angle detected and movement of robotic car	Average phase angle(A) for limit ± 20˚	Number of failed trials	Accuracy (N*10)%
1.	0˚ or 360˚ and Forward movement	- 12˚to + 14.93˚ or 342.5˚to 357.3˚	1*+1#	80% (8/10)
2.	90˚ and left movement	71.2˚ to 106.4˚	2*+1#	70% (7/10)
3.	180˚ and right movement	160.7˚ to 206.8˚	2#	80% (8/10)
4.	270˚ and Stop	253.3˚ to 287.4˚	2*+1#	70% (7/10)

Results:

The authors in [2] achieved synchronicity between the movements of both the simulated and the real robot car, and an average accuracy of 75% for phase detection. The uniqueness of this work is that, Hilbert Transform (HT) is applied to simulated EEG signal for phase extraction to control both simulated and real time robotic car simultaneously using LabVIEW and NI MyDAQ as a medium of interface. Upon phase identification, translational commands are then directed to robotic car wirelessly with the help of Radio Frequency (RF) transmission module working with a frequency of 434MHz. The commands are also passed to simulated robotic car in LabVIEW.

In paper [9] In this work, the SSVEP-based BCI consists of the SSVEP visual stimulus sources presented on a computer screen, EEG signal acquisition unit and processing unit. We use two flickering frequencies of 8 Hz and 10 Hz as SSVEP visual stimulus sources and use non-invasive BCI to obtain the SSVEP EEG signals. According to the result of the fine test with different analysis time lengths, they choose 3 s as the analysis time length of SSVEP signals. They use canonical correlation analysis (CCA) method to classify SSVEPs and the overlap time windows voting (OTWV) method to improve the classification accuracy, which is training- free and used to control a vehicle outdoor. The driver's intentions (moving or braking) are extracted by analyzing the frequency features of SSVEP signals. The BCI sends a moving command or a braking command to the vehicle according to the classification results. Since repeated moving or braking commands are invalid for controlling the vehicle, there is no need for the driver to continuously focus on the stimulus if the vehicle

stays in the desired state.

EEG acquisition unit

The device g.USBamp of g.tec medical engineering GmbH (Austria) was used as the bio-signal amplifier, which allows 16-channel bio-signal acquisition. The sampling frequency of the EEG signals was 256 Hz per channel. In SSVEP-based BCIs, channels at the occipital and parietal (visual cortex) area are always selected to record the SSVEPs. Subjects were asked to wear a special cap with fixed electrodes, and the SSVEP signals were collected from Oz, O1, O2, POz, PO3 and PO4, according to the international 10/20 system The ground electrode of g.USBamp was FPZ, positioned on the forehead, while the reference electrode was placed on the right earlobe.

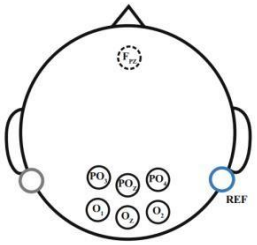

Preprocessing of EEG signals:

A 50-Hz notch filter and a Butterworth band pass filter were used to filter the power line interference and the high frequency noise. The Butterworth band-pass filter was used to extract EEG signals with frequencies between 5 and 60 Hz. A comparison between the raw EEG signals and the filtered EEG signals using Butterworth band-pass filter is shown. In this figure, the EEG signals were collected from Oz, O1, O2, POz, PO3 and PO4. Data from the 3-s EEG signals were segmented for noise removal.

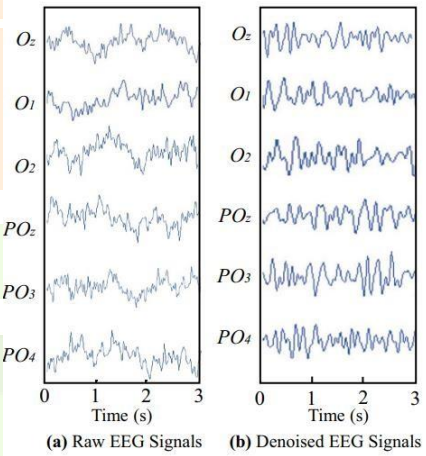

Fig:4

Methods used:

CAA

CCA method is used to classify SSVEPs by comparing the correlation between the collected SSVEP signals and each stimulus frequency. CCA is a statistical method, which has been traditionally and widely used to analyses relationships between two sets of variables in various Fields . The objective of CCA is to analyses the degree of correlation between two data sets by finding their transformed variants with the highest correlation by calculating their correlation coefficient. Two data sets are more relevant if their correlation coefficient is higher. The principle of the CCA method is described as follows. Given two data sets X and Y, CCA attempts to find a pair of vectors Wx and Wy that maximize the correlation between linear combinations of x and y, where x and y are calculated as:

$$x = X^T W_x$$

$$y = Y^T W_y$$

[equation 10]

In addition, x and y are known as canonical variates, which are uncorrelated in each data set and have zero mean and unit variance. Wx and Wy are the canonical coefficient vectors. rho is the correlation coefficient of x and y, and can be calculated as follows:

$$\rho = \max(corr(x,y)) = \max\left(\frac{Cov[x,y]}{\sqrt{Var[x]Var[x]}}\right) = \max\left(\frac{E[x^T,y]}{\sqrt{E[x^Tx]E[y^Ty]}}\right) = \max\left(\frac{E[W_x^TXY^TW_y]}{\sqrt{E[W_x^TXX^TW_x]E[W_y^TYY^TW_y]}}\right)$$

[equation 11]

Var, Cov and E represent the variance, the covariance and the expectation, respectively. The cross correlation

$$C_{X,Y} = E(XY^T)$$

$$C_X = E(XX^T)$$

$$C_Y = E(YY^T)$$

matrix of X and Y isdescribed a correlation.

[equation 12]

The collected SSVEP signals and a stimulus frequency are represented by two data sets, X and Y , respectively. X and Y are usedto calculate the CCA correlation coefficients. The CCA method can detect harmonic frequencies

$$Y = \begin{Bmatrix} \sin(2\pi ft) \\ \cos(2\pi ft) \\ \sin(4\pi ft) \\ \cos(4\pi ft) \end{Bmatrix}$$

[equation 13]

OTWV:

The OTWV method was used to improve the classification accuracy of the SSVEP signals. The OTWV method can improve the classification accuracy of the SSVEP signals without increasing the time length The classification accuracy of a 3-s SSVEP signals in a time window is p, and the classification accuracy using the OTWV methodis p′ .

$$p' = C_3^2p^2(1-p) + p^3$$

$$C_3^2p^2(1-p) + p^3 > p$$

$$p(2p-1)(p-1) < 0$$

$$p' = p^3 + p^2(1-p) + C_2^1p(1-p)^2$$ [equation 14]

Theoretically, with the OTWV method, a classification result is generated every 1 s in continuous signal processing, ignoring dataprocessing and transmission time. However, without the OTWV method, it takes at least 3 s to generate a classification result. Therefore, the OTWV method improves the generating rate of the classification results.

Experiment setup:

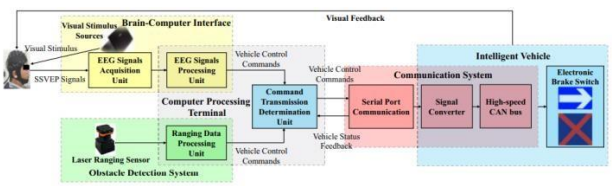

Fig: 5

Five healthy subjects aged between 21 and 27 participated in the experiment on a voluntary basis, and letters of consent were obtained from all of them. Some subjects had taken part in other earlier BCI experiments.

Two experiments were performed: (1) the simulated BCV experiment and (2) real vehicle controlling experiment. In the simulated vehicle controlling experiment, we verified the feasibility of the SSVEP-based BCI system to control a simulated vehicle in the virtual driving environment. In the real vehicle controlling experiment, we implemented the human-vehicle cooperative driving combining the BCV system with obstacledetection and verified the new controlling mode in the outdoor.
Subjects were asked to wear the EEG signal acquisition equipment and sat in front of the computer screen. The experiment was repeated four times for each subject. In each time, subjects were required to successively send ten commands, including five moving commands and five braking commands. Visual stimulus was given to the subjects in order to generate the commands. The same was done even in the real time also. with real obstacles present on the road. There was also laser detection present in the system in order to keep an alternate and incorporate safety if the system failed.

Results:

The Authors in [9] achieved 92% accuracy in simulated control and 90.68% in real time P300 potential motor imaginary SSVEP signals are used and EEG signals of 30-60hz are used CAA method are used to classify the signals OTWV method is used along with CCA in order it increase the classification accuracy further more when this two were used simultaneously an accuracy of 92.7% was achieved.

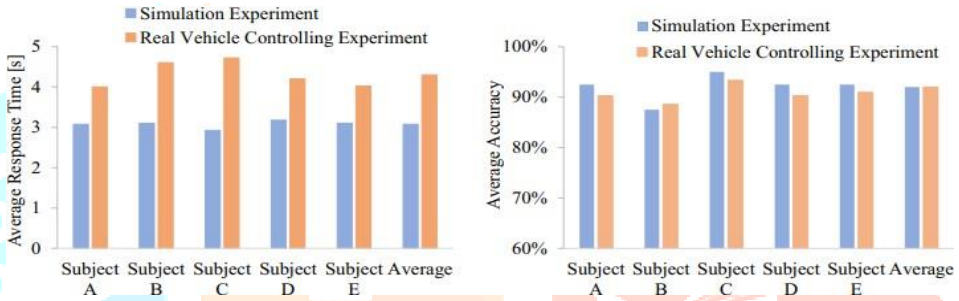

Fig: 6

In paper [12]

The Authors in [12] conducted five indivual experiments In which The subjects were told to perform different task the first task was to keep the car on an infield course, using “left” and “right” patterns for steering only. The velocity was set to 2 meters per second. In the second experiment the driving person had to control throttle and brake in addition to the steering commands for leftand right. The car was now able to accelerate from 0 to 3 meters per second. In third experiment to check the lateral error to the lane at higher speeds, we designed another track with long straight lanes and two sharp corners. The velocity was fixed to 5 meters per second. Further in the fourth experiment the response time of the test person. The test person received different commands, such as “left”, “right”, “push” or “pull” from another person and had to generate the corresponding brain pattern. Lastly they tested the second module, the Brain Chooser. Here, at intersections, the operator was asked to decide for the left or the right route. Then the test person had about ten seconds to decide for left or right direction. The overall accuracy was around 26% when all the five experiments were combined. Though the classification achieved a 90% effectiveness but the implementation did not reach the expected mark therefore BCI is little difficult to control steering of the vehicles.

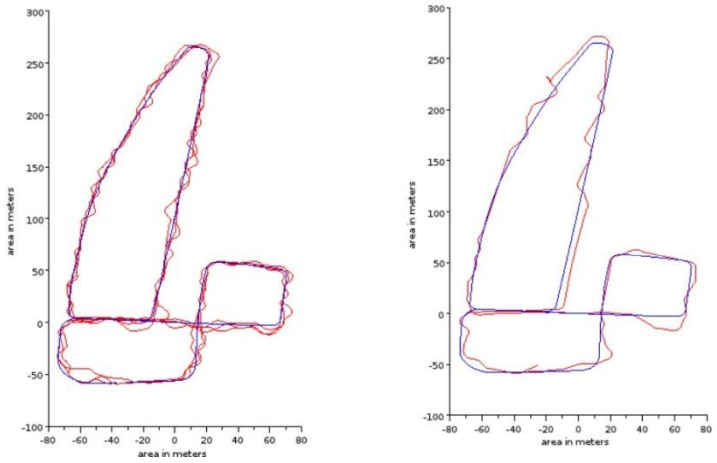

Fig: 7

	2s or less	2 - 5 s	5 - 10 s	10 s or more	falsely class.
percent	26 %	36 %	10 %	9 %	20 %

The Authors In [13]

The writer in reference [13] carried out the experiment using P300 BCI, with an SSVEP BCI confirmation component. The destination selection system operates according to the following protocol. Using the P300 BCI, users first choose their preferred destination from a list of options. If the chosen option is what they want, they can then accept it using the SSVEP BCI; if not, they can reject it and choose again until the final choice is made or the allotted time for selection has passed. Intelligent vehicles would drive them to the bogus destination if the system produced a false destination. In this instance, once the car reaches the fictitious destination, the disabled might currently choose their intended destination again. To categories the signals, they employed linear discrepancy analysis and an accuracy of 90.68% was achieved in laboratory condition and an accuracy of 88.99% was achieved under driving condition.

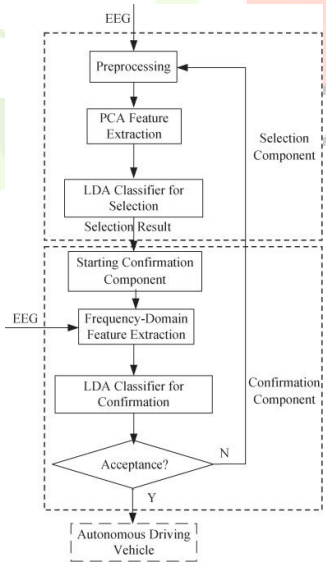

Fig: 8

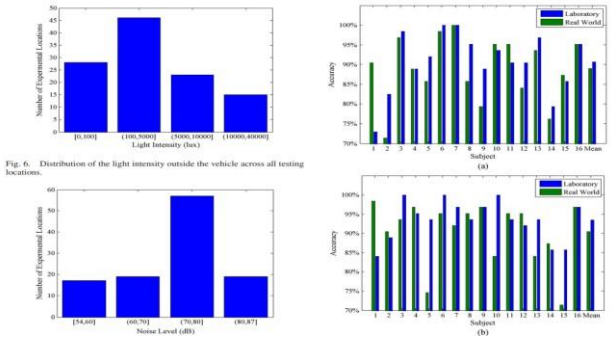

Fig: 9

CONLUSION:

Paper	Methods used	Accuracy Achieved
[1]	SVM,ELM,BELM,SBELM	76.3%, 77.1%, 77.8%, 78.5% respectively
[2]	Hilbert transform, LabView	75%
[9]	CAA, CAA+OTWV	91,68%, 92.7% respectively
[12]	Controlled steering	26%
[13]	LDA Classifier	Laboratory 90.68%, Outside Driving 88.99%

As from the above table we can see that CAA along with OTWV technique gives a higher range of classification of accuracy when compared to other classification technique as we can see LabView also gives a good amount of accuracy of 75% and is very useful for real time application as it is simple and easily decodable. It has secured a lesser accuracy only because of the transform they have used there are many options that can be used increase the accuracy.

REFRENCE:

[1] Z. Jin, G. Zhou, D. Gao, and Y. Zhang, "EEG classification using sparse Bayesian extreme learning machine for brain–computer interface," Neural Comput. Appl., vol. 32, no. 11, pp. 6601–6609, 2020, doi: 10.1007/s00521-018-3735-3.

[2] LABVIEW BASED SIMULTANEOUS CONTROL OF SIMULATED AND WIRELESS CONTROLLED ROBOTIC CAR USING SSVEP SIGNAL 1 SANDESH R.S., 2 S. VENKATESH, 3GANESH RAGHUNATHAN

[3] U. Herwig, P. Satrapi, and C. Schönfeldt-Lecuona," Using the international 10-20 EEG system for positioning of transcranial magnetic stimulation." Brain topography, vol. 16, no. 2, pp. 95-9, Jan. 2003. [4] V. Jurcak, D. Tsuzuki, and I. Dan," 10/20, 10/10, and 10/5 Systems Revisited: Their Validity As Relative Head-Surface-Based Positioning Systems." NeuroImage, vol. 34, no. 4, pp.1600-11, Feb. 2007.

[5] William Speier, Corey Arnold, Nader Pouratian, 'Evaluating True BCI Communication Rate through Mutual Information and Language Models', Published: October 22, 2013 https://doi.org/10.1371/journal.pone.0078432

[6] Daly JJ, Wolpaw JR. Brain-computer interfaces in neurological rehabilitation. Lancet Neurol. 2008 Nov;7(11):1032-43. doi: 10.1016/S1474-4422(08)70223-0. Epub 2008 Oct 2. PMID: 18835541.

[7]"Patient-Specific Modeling of Deep Brain Stimulation", Cameron C. McIntyre, Neuromodulation, Second Edition http://dx.doi.org/10.1016/B978-0-12-805353-9.00012-7 © 2018 Elsevier Ltd.

[8] Birbaumer, N. Breaking the silence: Brain–computer interfaces (BCI) for communication and motor control. Psychophysiology2006, 43, 517–532

[9] A Brain-Controlled Vehicle System Based on Steady State Visual Evoked Potentials Zhao Zhang1 · Shuning Han2 · Huaihai Yi3 · Feng Duan4 · Fei Kang5 · Zhe Sun6 · Jordi Solé-Casals2,4,7 · Cesar F. Caiafa4,8 Received: 7 February 2022 / Accepted: 14 August 2022 /

Published online: 10 September 2022 © The Author(s) 2022

[10] Ensemble Learning Based Brain-Computer Interface System for Ground Vehicle Control December 2019 .

[12] Semi-Autonomous Car Control Using Brain Computer Interfaces Daniel Gohring, David Latotzky, Miao Wang, Ra ¨ ul Rojas
´ Artificial Intelligence Group Institut fur Informatik ¨ Freie Universitat Berlin, Germany

[13] A Brain–Computer Interface-Based Vehicle Destination Selection System Using P300 and SSVEP Signals February 2015 IEEE Transactions on Intelligent Transportation Systems 16(1):274-283 DOI:10.1109/TITS.2014.2330000